

Measurements of the $^{63}\text{Cu}(\gamma, n)$ and $(\gamma, 2n)$ Cross Sections*

R. E. SUND, M. P. BAKER,† L. A. KULL, AND R. B. WALTON‡
Gulf General Atomic Incorporated, San Diego, California 92112

(Received 12 August 1968)

The $^{63}\text{Cu}(\gamma, n)$ cross section was measured over the energy range from threshold to 25 MeV with a photon beam of 2.0% resolution which was produced by the in-flight annihilation of positrons. The (γ, n) cross section was found to have a maximum value of 75 ± 6 mb at about 17.1 MeV and an integrated value up to 25 MeV of 490 ± 40 MeV mb. No structure was observed in these measurements or in additional (γ, n) measurements which were made in the region of the peak of the giant resonance with 1.5% γ -ray resolution. The (γ, n) data from the present experiment were combined with the $(\gamma, n) + (\gamma, pn)$ data from Livermore to obtain the $^{63}\text{Cu}(\gamma, pn)$ cross section, which was found to have a maximum value of 15 ± 4 mb at about 23 MeV and an integrated value up to 25 MeV of 60 ± 15 MeV mb. In addition, the $^{63}\text{Cu}(\gamma, 2n)$ cross section was measured at three representative energies between threshold and 26 MeV. The maximum $(\gamma, 2n)$ cross section obtained was 10.0 ± 1.6 mb at 23.7 MeV. The results of the experiments are compared with previous measurements and with theory. A small bump in the $(\gamma, n) + (\gamma, pn) + (\gamma, 2n)$ cross section at about 23 MeV may possibly be attributed to an analog giant resonance.

INTRODUCTION

MEASUREMENTS of the photoreaction cross sections of copper in the energy region of the giant resonance are of interest for comparison with theoretical predictions for spherical nuclei¹⁻³ that are based on the dynamic collective theory of the nuclear photoeffect. The dynamic collective theory differs from the static hydrodynamic theory of giant dipole oscillations in that low-energy quadrupole surface motions are also treated.⁴ In the case of spherical nuclei, the quadrupole vibrations are coupled strongly to the dipole oscillations, with the result that the dipole strength is distributed mainly among four or five states within an interval of approximately 5 MeV. For many nuclei these states produce bumps in calculated photoabsorption cross sections. Available experimental data for spherical nuclei generally are in agreement with the gross features of the theoretical cross sections, and in some cases tend to verify the predicted structure in the giant resonance.¹

The (γ, n) cross section of copper is also of interest because it has served as a photonuclear cross-section standard and, as such, it provides a rather good gauge of the reliability of the photoneutron measurements performed over the years. The accuracy of absolute cross sections are of particular concern for dipole sum-rule comparisons. From the extensive surveys found in the literature,⁵⁻⁷ it is apparent that most of the results

of measurements for the (γ, n) cross sections of natural copper and the copper isotopes that were obtained with bremsstrahlung beams are considerably higher (~ 10 – 50%) than the results of measurements made with γ rays from the $^7\text{Li}(p, \gamma)$ reaction and the data obtained by Fultz *et al.*⁵ at Livermore with γ rays produced by the in-flight annihilation of positrons from an electron linear accelerator (LINAC). The measurements by the latter group were performed with a γ -ray energy resolution of 3%. Additionally, the photoneutron cross section of natural copper measured as a function of energy by Miller *et al.*⁸ with positron annihilation γ rays and the $^{63}\text{Cu}(\gamma, n)$ cross section measured at 20.5 MeV with $^3\text{H}(p, \gamma)$ γ rays by Del Bianco and Stephens⁹ are appreciably higher than the results of Fultz *et al.*⁵ Discrepancies between the various experimental data are usually much larger than the experimental errors quoted.

In the present work, the (γ, n) and $(\gamma, 2n)$ cross sections were measured using the activation analysis method of detection and almost monoenergetic γ rays produced by the in-flight annihilation of positrons. The (γ, n) data were obtained over the energy range from threshold to 25 MeV with an energy resolution of 2%, and, in a search for structure in the cross section, additional data were taken with 1.5% resolution over the peak of the giant resonance. The activation analysis method for the determination of the number of photoneutron events has the advantages that (1) the detection efficiency is independent of the neutron energy spectrum, which may vary with the energy of the bombarding photons, and (2) isotopic cross sections can often be obtained with normal elemental samples. Furthermore, the determination of the $^{63}\text{Cu}(\gamma, n)$ cross section by this method afforded the possibility of deriving the (γ, pn) cross section from the $(\gamma, n) + (\gamma, pn)$ cross sections of ^{63}Cu obtained by Fultz *et al.*⁵ Using a highly efficient neutron detector, they separated the

* Research supported in part by the U. S. Office of Naval Research under Contract No. Nonr-4024(00).

† Present address: University of Washington, Seattle, Wash.

‡ Present address: Los Alamos Scientific Laboratory, Los Alamos, N. M.

¹ M. G. Huber, M. Danos, H. J. Weber, and W. Greiner, *Phys. Rev.* **155**, 1973 (1967).

² H. Arenhovel and H. J. Weber, *Nucl. Phys.* **A91**, 145 (1967).

³ J. Le Tourneux, *Kgl. Danske Videnskab. Selskab, Mat.-Fys. Medd.* **34**, No. 11 (1965); J. Le Tourneux, *Phys. Letters* **13**, 325 (1964).

⁴ M. Danos and W. Greiner, *Phys. Rev.* **134**, B284 (1964).

⁵ S. C. Fultz, R. L. Bramblett, J. T. Caldwell, and R. R. Harvey, *Phys. Rev.* **133**, B1149 (1964).

⁶ S. Yasumi, M. Yata, K. Takamatsu, A. Masaie, and Y. Masuda, *J. Phys. Soc. Japan* **15**, 1913 (1960).

⁷ G. E. Coote, W. E. Turchinets, and I. F. Wright, *Nucl. Phys.* **23**, 468 (1961).

⁸ J. Miller, C. Schuhl, and C. Tzara, *Nucl. Phys.* **32**, 236 (1962).

⁹ W. E. Del Bianco and W. E. Stephens, *Phys. Rev.* **126**, 709 (1962).

$(\gamma, 2n)$ events from the (γ, n) and (γ, pn) events by a statistical analysis of the data.

PROCEDURES FOR CROSS-SECTION MEASUREMENTS

Measurements of Excitation Functions

The experimental arrangement used for these cross-section measurements is shown in Fig. 1. Approximately 1.5-MeV positrons and electrons produced by bombarding a water-cooled tungsten converter with the intense electron beam from the first section of the LINAC were focused into the following section of the accelerator. Either positrons or electrons from the converter were accelerated to the desired energy by adjusting the phase and power of the rf applied to the last two wave guides. After leaving the accelerator, the beam was energy analyzed by a 36° sector magnet, the field strength of which was measured with a NMR gaussmeter. The beam then passed through another 36° magnet and a 2.4-m-thick shield wall to a Be annihilation target. The 36° magnet system¹⁰ focused the beam into a spot which contained $\sim 95\%$ of the beam within a diameter of 1.27 cm at the position of the annihilation target. After passing through the annihilation foil, the beam was swept by a magnet through an angle of 45° into a Faraday cup. The charge collected on this cup served as the beam monitor. The charge measuring system consisted of a Keithley 418 micromicroammeter which was connected to the Faraday cup and a standard microampere current integrator which was linked to the voltage output of the Keithley through precision resistors. With a $135\text{-}\mu\text{A}$ (time-averaged) beam of 11-MeV electrons incident on the converter, a typical positron current at the annihilation target for 25-MeV positrons with an energy spread of $\sim 1.2\%$ was 3×10^{-10} A. The annihilation foil could be retracted by remote control to check for possible radiation produced in the beam tube system by scattered particles and to check that the foil did not interfere with the beam current measurements. The beam was aligned by steering it through a 1.27-cm hole in a retractable aluminum collimator located immediately in front of the Be foil.

Positron-annihilation γ rays emanating from the Be foil passed through a lead collimator which was 3.65 cm in diam and extended 105 cm from the Be foil. A tungsten insert was placed at the exit of the collimator to reduce beam transmission through the collimator edges. Samples to be irradiated with the γ -ray beam were mounted in carrier cylinders which were inserted into a sample changing wheel located behind the collimator. The samples for this study were 4.45-cm diam, 1.02-cm thick disks of elemental copper. In the $^{63}\text{Cu}(\gamma, n)$ and $^{63}\text{Cu}(\gamma, 2n)$ measurements the samples were irradiated for a time approximately equal to the half-lives of the reaction products, 9.8 min for ^{62}Cu and 3.3 h for ^{61}Cu . The charge from the Faraday cup was fed to the

¹⁰ K. L. Brown, Rev. Sci. Instr. 27, 959 (1956).

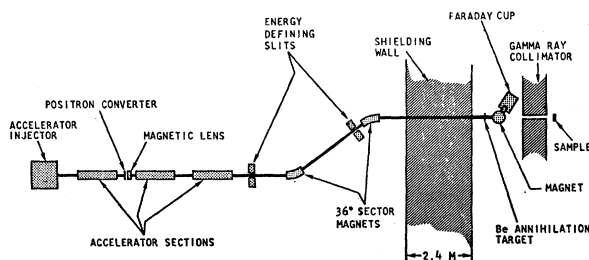


Fig. 1. Schematic drawing of the accelerator, positron-beam translating system, and γ -ray monochromator.

current integration system which was operated as a leaky current integrator¹¹ to compensate automatically for beam fluctuations during irradiations. After an irradiation, the same was transferred automatically by a fast pneumatic system to the data acquisition area and placed between two 12.7-cm-diam NaI detectors which were 7.6 and 14.7 cm long. These were used to detect coincidences between the 511-keV γ -ray photopeaks which resulted from the annihilation of the positrons from ^{62}Cu and ^{61}Cu . The effect of the bremsstrahlung tail in the photon spectrum produced by positrons striking the Be foil was evaluated by repeating each measurement with a beam of electrons having the same energy as the positrons. The difference between the activities produced by the positron and electron irradiations was the activity generated by positron annihilation photons.

Photon-Flux and Energy-Resolution Determinations

In the present work, the absolute flux of positron annihilation γ rays used to obtain photoreaction cross sections was computed with the modified version of the Monte Carlo code of Cardman and Owens.¹² Several flux measurements were performed to check the computed results.

The Cardman-Owens code takes into account the dependence in the annihilation process of the cross section and the photon energy on the angle between the positron and the γ ray, the multiple scattering and energy loss of positrons in the annihilation target, and the finite angular acceptance of the collimation system. Results computed with this code agree very well with the analytical calculations of Elliott and Katz,¹³ which include all of the above effects. In a modified version of their Monte Carlo code, Cardman and Owens also took into account the effects of the energy spread, lateral extent, and angular divergence of the positron beam incident on the annihilation target.

The code of Cardman and Owens was adapted for our computer and checked against the test cases given by the originators. Furthermore, the photon intensity

¹¹ S. C. Snowden, Phys. Rev. 78, 299 (1950).

¹² L. S. Cardman and R. O. Owens, Yale Internal Report No. EAL 2726-39 (unpublished).

¹³ R. Elliot, K. Lukan, D. Lobb, and L. Katz, Saskatchewan Accelerator SAL Report No. 3, 1964 (unpublished).

was computed as a function of annihilation foil thickness, and the zero-thickness extrapolations agreed well with the values computed from the fundamental annihilation cross section.¹⁴ Calculations of the number of photons per positron were then performed for several positron energies between 10.5 and 25.5 MeV for the standard geometry and beam conditions used for the cross-section measurements: a 0.0508-cm-thick Be annihilation foil, a 1° γ -ray collimator angle θ_e , a distance of 105 cm from the annihilation foil to collimator exit, a positron beam which had 95% of its intensity within a 1.27-cm-diam area and also 95% of its intensity within a divergence angle of 0.17° , and a calculated positron beam resolution of 1.2%. The calculated number of annihilation photons per positron incident on the foil versus the total positron energy E_{β^+} (including rest energy) are presented in Fig. 2. The error bars on the data points reflect the statistical uncertainties of the Monte Carlo calculations. The application of these calculations to our experimental setup is further uncertain by about $\pm 3\%$ due to nonuniformities in the Be foil thickness. Since the number of photons per positron striking the Be foil is not very sensitive to the shape of the positron energy spectrum or to small changes in the spatial distribution of the positron beam, the errors in the calculated flux which resulted from the inexact duplication of these experimental conditions

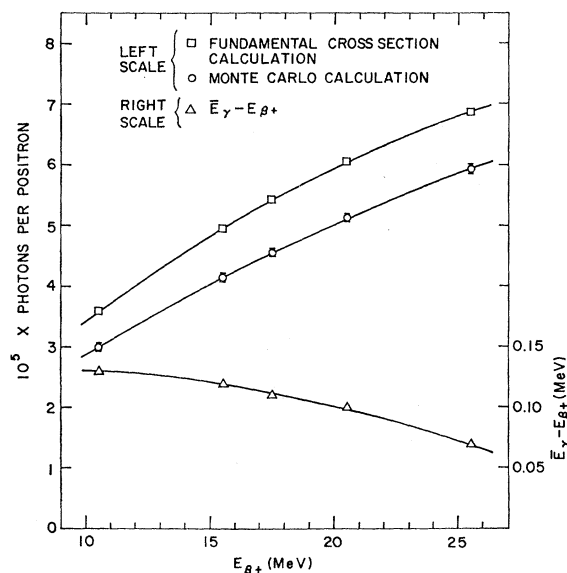


FIG. 2. The number of annihilation photons per positron incident on the Be foil versus the total positron energy E_{β^+} , as calculated with the Monte Carlo code for the conditions used in the cross-section measurements. For comparison we show the flux calculated from the fundamental annihilation cross section, neglecting multiple scattering of the positrons in the Be foil and the spatial extent of the positron beam. In addition, the difference between the mean photon energy \bar{E}_{γ} and E_{β^+} is given as a function of E_{β^+} .

¹⁴ J. M. Jauch and F. Rohrlich, *Theory of Electrons and Photons* (Addison-Wesley Publishing Co., Reading, Mass., 1955).

were small. For comparison, the flux calculated using the fundamental annihilation cross section and neglecting both the multiple scattering of positrons in the Be foil and the spatial extent of the positron beam is also given. The Monte Carlo program also computes the annihilation photon spectrum and the mean photon energy \bar{E}_{γ} . In Fig. 2 the difference between \bar{E}_{γ} and E_{β^+} is plotted as a function of E_{β^+} for the beam conditions and geometry used for the cross-section measurements. A typical difference between \bar{E}_{γ} and the energy of the annihilation peak (at the midpoint between the half-heights of the peak) is 0.03 MeV at $\bar{E}_{\gamma} = 15$ MeV.

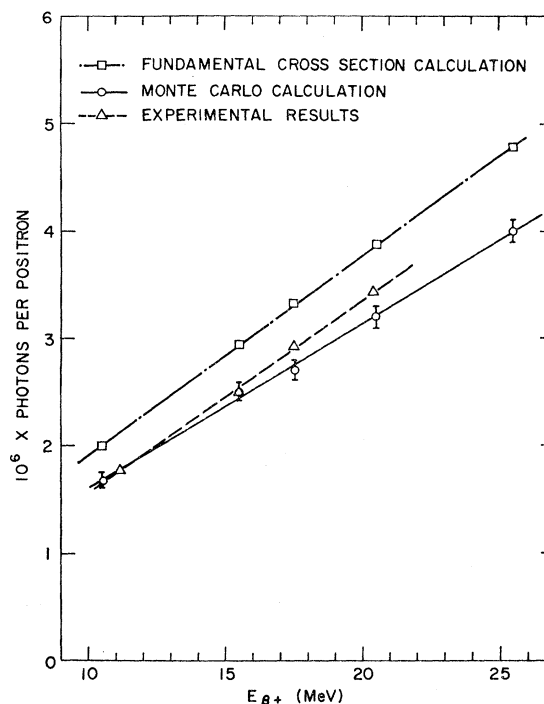


FIG. 3. The number of annihilation photons per positron incident on the Be foil versus the total positron energy, as calculated with the Monte Carlo code for the conditions used in the flux measurements. For comparison, we show the experimental results and also the results of the flux computed with the fundamental annihilation cross section and neglecting multiple scattering of the positrons and the spatial extent of the positron beam.

Additional calculations were performed for the geometry used in the experimental determinations of the flux. In this case the distance from the annihilation target to the collimator exit was 238 cm, θ_e was 0.23° , and all other parameters were the same as those given above. Figure 3 shows the results of the flux computed with the Monte Carlo code and, for comparison, the flux computed using the fundamental annihilation cross section and neglecting multiple scattering of the positrons and the spatial extent of the positron beam. The statistical uncertainties in the Monte Carlo calculations are about $\pm 3\%$, and the comparison of these data to the experimental results is further uncertain by the

$\pm 3\%$ due to nonuniformities in the thickness of the Be foil.

Measurements of the photon flux were performed at four energies with a 12.7-cm-diam by 14.7-cm-long NaI crystal. Very small positron and electron beam currents ($\sim 10^{-12}$ A) were used in these measurements in order to keep the pulse pile-up rate at a small level that could be accurately evaluated. The lower limit of usable beam current was determined by the magnitude of the dark current of the charge collection system. For these measurements the dark current was always less than 1.5% of the beam current, and the data were corrected for this effect. The NaI crystal was located behind a 1.90-cm-diam tungsten collimator, the exit

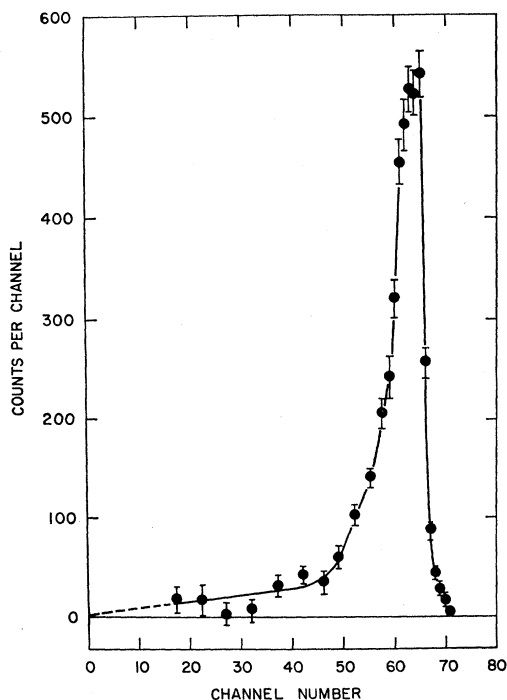


Fig. 4. NaI spectrum of 11.3-MeV positron annihilation γ rays after subtraction of the electron data from the positron data.

of which was 238 cm from the Be foil. This small collimation angle was selected to minimize the escape of radiation from the sides of the NaI crystal and to help reduce pulse pile-up in the detection system. A 46-cm-long cylinder of aluminum was placed between the Be foil and the detector to reduce the intensity of the bremsstrahlung radiation relative to the intensity of positron annihilation γ rays. To check that the optical alignment of the detection system coincided with the true photon-beam axis, counting rate measurements were performed with the detector and its collimator translated horizontally and vertically from the optically determined beam axis.

The experimental data consisted of pulse-height spectra produced by positrons and electrons impinging

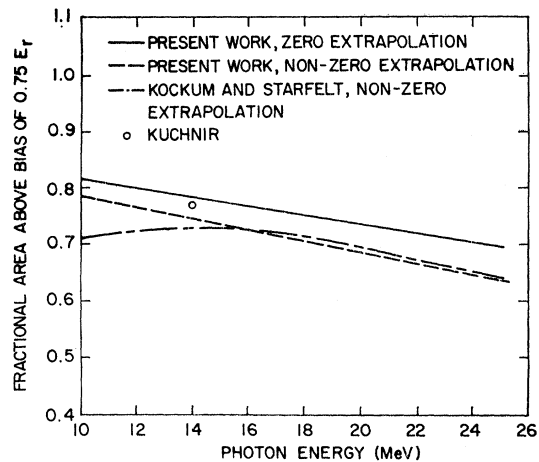


Fig. 5. The fraction of the area of the NaI response function above 75% of the pulse amplitude corresponding to full-energy deposition of the γ rays versus the γ -ray energy. The present results with zero- and nonzero-tail extrapolation, the results for a 12.7-cm-diam by 14.7-cm-long NaI crystal derived from the measurements of Kockum and Starfelt (Ref. 15), and the results of Kuchnir (Ref. 16) at 14 MeV for a 14.7-cm-diam by 10.2-cm-long NaI detector are shown.

on the Be foil, and the flux of positron-annihilation γ rays was derived from the difference between these spectra. The absolute numbers of bombarding positrons and electrons were determined from measurements of the charge collected by the Faraday cup during the runs. An example of the net pulse-height-distribution data, which were obtained for a positron-annihilation photon energy of 11.3 MeV, is presented in Fig. 4. In principle, the measurements should have yielded the full response functions of the detector for monoenergetic γ rays; however, because the subtraction of the bremsstrahlung pulse-height spectra produced large uncertainties at low pulse amplitudes, the response functions had to be extrapolated to zero pulse height. For the magnitude of the response function at zero pulse height we used the theoretical intercept, which for practical purposes is essentially zero.^{9,15} Our measurements at 17.5 and 20.5 MeV are consistent with this extrapolation, and our results at 11.3 and 15.6 MeV are in better agreement with this extrapolation than with the nonzero extrapolation proposed by Kockum and Starfelt.¹⁵ A plot of the fraction of the area of the response function above 75% of the pulse amplitude corresponding to full-energy deposition of the γ ray is given as a function of E_γ in Fig. 5. Results of the present investigation with both zero and nonzero tail extrapolations, together with the results derived from the measurements of Kockum and Starfelt for a 4.5-cm-diam collimator and a 12.7-cm-diam by 14.7-cm-long NaI crystal, are shown. The single point at $E_\gamma = 14$ MeV represents the result obtained at the University of Illinois with a beam of monoenergetic photons, a γ -ray collimator of roughly 6×10 cm, and a 14.7-cm-diam by 10.2-cm-long NaI

¹⁵ J. Kockum and N. Starfelt, Nucl. Instr. 4, 171 (1959).

crystal.¹⁶ This result is expected to be lower than the present measurements because of the smaller crystal size and the larger area of collimation in the University of Illinois measurements. The upper curve was used in the present flux determinations.

The experimental data were corrected for the attenuation by the aluminum beam hardener. Small corrections (typically less than 1%) were applied to the data to account for the Compton in-scattering of photons by the aluminum beam hardener, the transmission of photons through collimator edges, and the effect of emission of secondary electrons from the Faraday cup. The last correction is discussed later. The total γ -ray detection efficiency of the NaI crystal was calculated as a function of energy using the absorption coefficients for NaI given by Hubbell and Berger.¹⁷ In these calculations nuclear absorption by NaI and γ -ray interactions in the crystal housing which deposited electron-positron pairs and Compton γ rays in the NaI crystal were taken into account. The results of the flux measurements are presented in Fig. 3. The largest error in these results, $\pm 6\%$, is the uncertainty in the NaI response function. The error in the flux caused by the uncertainty in the calculated attenuation of the photon beam by the Al beam hardener is $\pm 4\%$. Statistical uncertainties and other errors in this measurement were relatively smaller. The measured fluxes agree well with those obtained with the Monte Carlo code at the lower energies, but are higher by about 9% at 20.5 MeV. This difference is well within the combined errors of the experiment and the calculations.

Since the flux measurements were performed in a geometry which was different from that utilized for measurement of the (γ, n) and $(\gamma, 2n)$ excitation function of ^{63}Cu , additional measurements were undertaken to verify the Monte Carlo calculations of the intensity of photons striking the copper samples (see Fig. 2). These tests consisted of measuring at annihilation photon energies of 17.2 and 19.8 MeV the ratio of the number of photons contained within a 3.65-cm-diam aperture at 105 cm from the Be foil (the geometry used for the cross-section measurements) to the number contained within the same aperture at 238 cm (the position at which the flux was measured with the NaI detector). The ratios were determined by measuring the number of $^{63}\text{Cu}(\gamma, n)$ events produced by the positron annihilation γ rays in copper samples placed behind collimators located at the two distances. Both of the experimentally determined ratios agreed with the calculated ratios to within 1.5%, which is well within the limits of the errors of about $\pm 4\%$ in both the experimental and calculated values. The computer calculations indicate that at the 238-cm location and for energies between 10 and 25 MeV, the average flux

¹⁶ F. T. Kuchnir (private communication); from F. T. Kuchnir, Ph.D. thesis, University of Illinois, 1965 (unpublished).

¹⁷ J. H. Hubbell and M. J. Berger, Natl. Bur. Std. (U. S.) Report No. 8681, 1966 (unpublished).

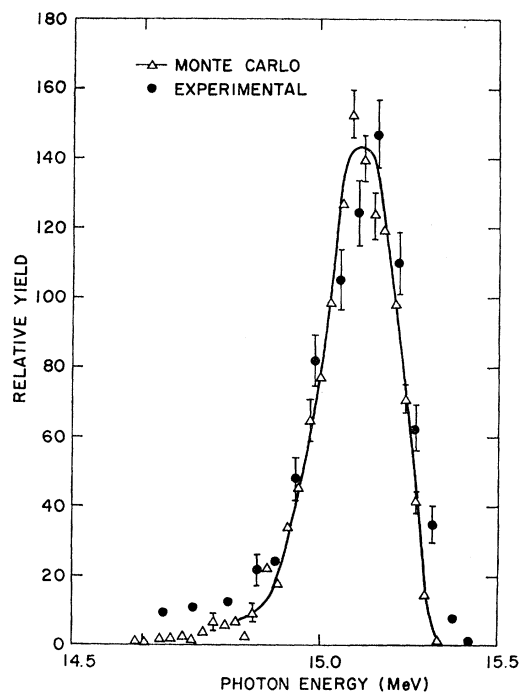


FIG. 6. Spectrum of annihilation γ rays determined by elastic scattering from the 15.1-MeV level in ^{12}C . The Monte Carlo calculation of the annihilation spectrum is shown for comparison.

per unit solid angle for a 1.9-cm aperture is $\sim 1\text{--}4\%$ larger than that for a 3.65-cm-diam aperture, i.e., the γ -ray beam is almost isotropic at 238 cm for aperture diameters less than 3.65 cm, and a negligible error should exist in the computer results for the ratio of the fluxes at 238 cm for the two aperture sizes. Thus the agreement of the experimental and calculated ratios of fluxes at the two distances from the Be foil and the agreement, within errors, of the measured and calculated fluxes at the 238-cm distance indicate that the calculations of the photon intensity given in Fig. 2 are valid within the error bars for the photon energy range covered in the present cross-section measurements.

The energy resolution of the photon beam used for the cross-section measurements was obtained by measuring with the 12.7-cm-diam by 14.7-cm-long NaI crystal the intensity of 15.1-MeV resonance fluorescence γ rays from a carbon sample as a function of the energy of the positron beam. The results of measurements of the energy spectrum of photons contained within the 1° collimator used in the cross-section measurements and produced by positrons with an energy resolution of $\sim 1.2\%$ striking a 0.051-cm-thick Be foil are shown in Fig. 6. The energy resolution of the photon beam, derived from these data, is 2% (full width at half-maximum). Also shown in this figure is the spectrum calculated with the Monte Carlo code. The differences in the measured and calculated spectra probably result from the difference in the shape of the actual energy spectrum of the positron beam and the rectangular

shape used in the code. The photon-beam energy resolution was also measured for a 0.025-cm-thick Be foil, a positron energy resolution of about 1.0%, and a collimation angle of 1° . For this case the photon-beam energy resolution was found to be 1.5%. These resonance fluorescence measurements also provided a precise energy calibration for the photon beam.

Efficiencies of NaI Crystals for Detecting ^{62}Cu and ^{61}Cu Positron Activities

The efficiency of the NaI crystals for detecting 511-keV γ rays resulting from the annihilation of positrons from a sample was determined with sources of ^{18}F (half-life = 110 min) which were intercalibrated with a NBS ^{22}Na standard source. The ^{22}Na source was not used directly for the calibration of the system because of the interference produced by the coincidence summing of the 511-keV annihilation γ rays and the 1.275-MeV γ rays accompanying the positron decay of ^{22}Na . Samples containing ^{18}F were prepared by irradiating a stack of thin, 0.63-cm-diam Teflon foils with bremsstrahlung having an endpoint energy below the $^{12}\text{C}(\gamma, n)$ threshold. The geometry for this irradiation was such that the positron activity per unit mass of the Teflon was uniform, within very small errors, over the area and depth of the foils. The positron activity of the foils was measured relative to the positron activity of the ^{22}Na source by coincidence counting the 511-keV annihilation γ -ray photopeaks in a geometry consisting of the 12.7-cm-diam NaI crystals separated by 154 cm and with the source located midway between them. Because there is no angular correlation between the 1.275-MeV γ rays and the annihilation γ rays, the rate of coincidences involving the 1.275-MeV γ rays in this expanded geometry was less than 1% of the annihilation γ -ray coincidences. The thickness of the source holder was sufficient to stop the positrons and was adjusted so that the over-all attenuation of the annihilation radiation was the same for the ^{22}Na and ^{18}F sources.

After the measurement of the activity of the ^{18}F foils, the NaI crystals were restored to the normal configuration used for the cross-section measurements, and one of the ^{18}F foils, the activity of which was determined relative to the batch of foils by weighing, was used to measure the efficiency of the detector. To account for the distributed source effects in the copper samples, the ^{18}F foil was inserted between copper disks which simulated the actual samples, and measurements of the counting rate were performed as a function of axial and radial position of the foil within the assembly of copper disks. The efficiency for coincidence counting the annihilation γ rays with the source located at the center of the sample was 0.136 ± 0.004 . The variation of the efficiency with radial position ranged from 3 to 6%, depending on the axial position, and the efficiency of the detection system with the source centered on

the cylindrical axis of the sample varied with axial position by 8%. The correction accounting for the distributed source was calculated by weighting these variations with the angular distribution of the annihilation photon beam and with the attenuation of this beam by the sample; the variation in this correction with γ -ray energy was negligibly small. The resulting efficiency was 3% lower than that measured with the source centrally located in the copper sample.

As an independent check on the efficiency of the system, the ^{18}F foil which was used with the normal configuration of the NaI detectors was calibrated directly against the standard ^{22}Na source with a Ge(Li) detector. The ^{18}F foil and the ^{22}Na source were positioned at the same distance from the Ge(Li) detector; at this distance the coincidence summing between the 511-keV γ rays and the 1.275-MeV γ rays from the ^{22}Na source removed only 0.3% of the counts from the 511-keV photopeak. The result of this measurement agreed, within error bars, with that given above.

As a check on the intensity quoted for the NBS source, an independent measurement of the intensity of this source was performed at Los Alamos Scientific Laboratory with a 28-cm-diam by 28-cm-long NaI well counter, and a sum-coincidence scheme was used to derive the absolute intensity from the data. The result obtained was 5.6% higher than the quoted value. Since the uncertainties of the NBS number and the Los Alamos measurement were both $\pm 1\%$, the average of these intensities was used, and an uncertainty of $\pm 2.8\%$ was assigned to this average. The efficiency given above was determined with this average. As a further check on the ^{22}Na absolute source strength, the absolute source strength of the ^{18}F foils was obtained independently by counting the ^{18}F activity as a function of foil thickness with a 4π β -ray counter. The result for the ^{18}F source intensity agreed to within 1% of the average number obtained using the ^{22}Na source, and the error on the ^{18}F measurement was $\pm 3\%$.

To obtain the final efficiencies for detecting the ^{61}Cu and ^{62}Cu positron activities with the NaI coincidence system, the efficiency given above had to be corrected for effects caused by bremsstrahlung generated by the stopping of the positrons in the copper samples and also for the γ rays accompanying the positron decay. The sum pulses produced by simultaneous detection of these photons and the annihilation radiation had to be taken into account to obtain the true number of 511-keV photopeak coincidences. The effect of the sum pulses in the efficiency measurements with ^{18}F was negligible because the positron endpoint energy is only 0.65 MeV and no γ rays are emitted in the decay of ^{18}F . ^{62}Cu is essentially a pure positron emitter, but a significant number of sum pulses resulted from positron bremsstrahlung since the positron endpoint energy is 2.9 MeV. In the case of ^{61}Cu , the positron endpoint energy is 1.21 MeV and approximately 15% of the

positron emissions are accompanied by γ rays. The net losses of photopeak coincidence counts caused by these summing effects, which were calculated from measured coincidence pulse-height spectra, amounted to 5 and 9% for ^{62}Cu and ^{61}Cu , respectively. The resulting absolute efficiencies for counting the positron activity from ^{62}Cu and ^{61}Cu were 0.125 ± 0.005 and 0.120 ± 0.006 , respectively.

RESULTS

The $^{63}\text{Cu}(\gamma, n)$ yields generated by the positron and electron beams incident on the 0.051-cm-thick Be foil are shown in Fig. 7. The energy scale in the figure is that of the annihilation photons, and the energy resolution of this beam was 2%. The data above 19.8 MeV include results from two independent measurements which were made several months apart as a check on reproducibility. The ^{62}Cu activation yields which are given in this figure were measured for 10 min beginning 1 min after the end of an irradiation. The backgrounds that were caused by the 12.9-h ^{64}Cu activity from $^{65}\text{Cu}(\gamma, n)$ reactions and the 3.3-h ^{61}Cu activity from $^{63}\text{Cu}(\gamma, 2n)$ reactions were negligibly small.

Because the bremsstrahlung tail of the photon spectrum produced by positrons with energies greater than about 21 MeV accounted for a large portion of the copper activity, it is evident that any small systematic errors in the evaluation of the bremsstrahlung-produced activity could cause much larger errors in the net activity obtained for the positron annihilation photons at the higher bombarding energies. To evaluate the accuracy of the procedure for subtracting the bremsstrahlung activity, the $^{63}\text{Cu}(\gamma, n)$ activities produced by 27-MeV positrons and electrons incident on a 0.001-cm-thick gold foil were measured and compared. Because almost all of the ^{62}Cu activity produced by 27-MeV positrons incident on Be is due to bremsstrahlung and since the ratio of the bremsstrahlung intensity to annihilation intensity for gold is ~ 20 times that for

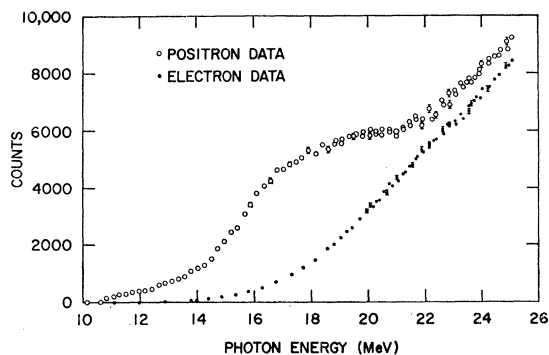


Fig. 7. The $^{63}\text{Cu}(\gamma, n)$ yield (per current integration monitor) produced by the positrons or electrons incident on the Be foil. The energy scale is that of the annihilation photons. The data above 19.8 MeV include results from two independent runs made several months apart as a check on reproducibility. The error bars for the low-energy data are too small to show.

Be, the activities produced by 27-MeV positrons and electrons striking the gold foil should have differed by less than 0.5%. The measurements showed that the activity produced by the electrons was 3.6% higher than that produced by the positrons. The over-all accuracy of the bremsstrahlung subtraction procedure was also obtained at 20 MeV by measuring the pulse-height spectra produced in a NaI crystal by photons from positron and electron bombardment of a 0.0006-cm-thick Ta foil. The experimental arrangement for this measurement was the same as that used for the flux measurements. This measurement showed that the electron data were higher than the positron data by

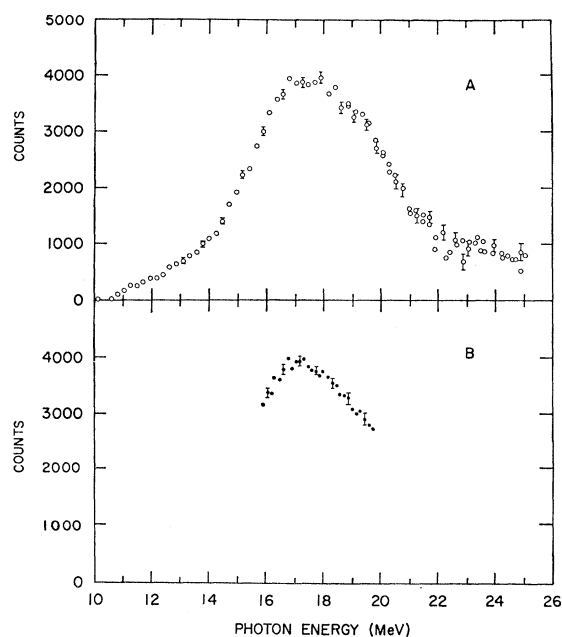


Fig. 8. (A) The $^{63}\text{Cu}(\gamma, n)$ yield versus annihilation γ -ray energy for 2% γ -ray resolution. This yield is the difference between the positron and electron data shown in Fig. 7. (B) The $^{63}\text{Cu}(\gamma, n)$ yield versus annihilation γ -ray energy for 1.5% γ -ray resolution. These data were approximately normalized to the data in Fig. 8(A).

2.1%. Since the electronic components used in the current integration system were stable to within $\frac{1}{2}\%$ and were routinely checked with a precision current source (Keithley 261-picoampere source), these components were not believed to be the source of the measured systematic errors in the bremsstrahlung subtraction procedure. Additionally, the error caused by small differences in the positron and electron beam spot sizes was estimated to be negligibly small. Since the Faraday cup used in this experiment was smaller than that recommended by Tautfest and Brown,¹⁸ we concluded that the observed errors were most likely due to the emission of secondary electrons from the

¹⁸ K. W. Brown and G. W. Tautfest, *Rev. Sci. Instr.* **27**, 696 (1956).

Faraday cup. An expression for the energy dependence of the correction for this effect was derived and normalized to the two experimentally determined values. All of the positron and electron activation data shown in Fig. 7 and the following figures were corrected for the Faraday-cup error, and the error bars shown in the figures include the uncertainties in the Faraday-cup correction as well as the statistical uncertainties in the activation measurements.

The $^{63}\text{Cu}(\gamma, n)$ yield from positron annihilation photons, which was obtained by subtracting the yield curves given in Fig. 7, is presented in Fig. 8(A). Because of interest in possible structure in the cross sections of spherical nuclei, measurements of the $^{63}\text{Cu}(\gamma, n)$ yield were also performed over a portion of the giant resonance with a photon beam having an energy resolution of 1.5%. These results, given in Fig. 8(B), indicate that the cross section varies smoothly

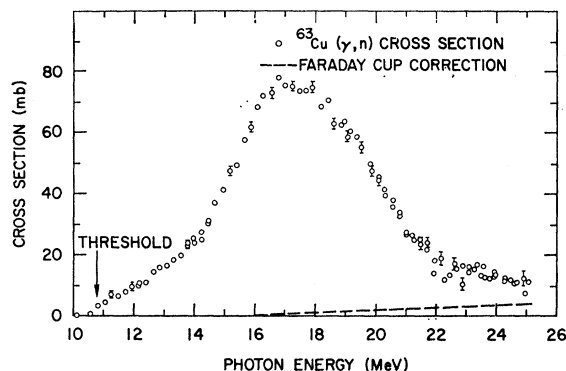


FIG. 9. The $^{63}\text{Cu}(\gamma, n)$ cross section versus photon energy for 2% γ -ray resolution. The data shown were corrected for the emission of secondary electrons from the Faraday cup, and the magnitude of this correction is also shown. See text for discussion of errors.

with photon energy for a photon beam resolution of 1.5%.

The present results for the $^{63}\text{Cu}(\gamma, n)$ cross section obtained as a function of photon bombarding energy and with a beam energy resolution of 2.0% are given in Fig. 9. The data points have been corrected for the positron-electron difference caused by the emission of secondary electrons from the Faraday cup, and the magnitude of this correction is given by the dashed curve in the figure. Corrections were also applied to the data for the attenuation of the positron annihilation γ rays in the Cu samples and for the small activity produced by the second interaction of photons which had initially been Compton scattered within the sample. This last correction was about 3% at 25 MeV and was less than 1% for energies below 20 MeV. The error bars shown in Fig. 9 represent the statistical uncertainties in the activation measurements and the uncertainties in the determination of the positron-electron difference caused by the emission of secondary elec-

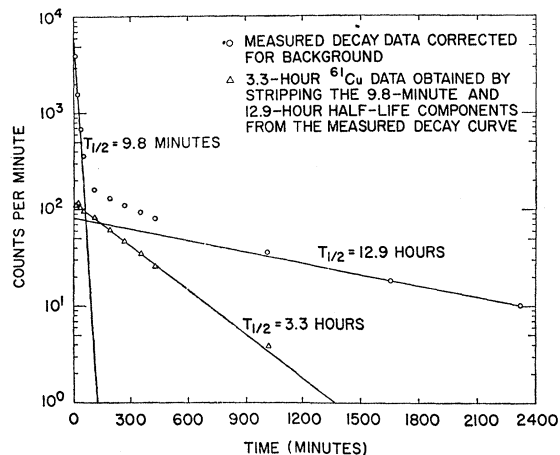


FIG. 10. Counting rate versus time for a copper sample after an irradiation with 25.6-MeV positrons striking the Be annihilation foil. The error bars for the circular data points are smaller than the circles in every case. The three components which result from the least-squares fit are shown and the 3.3-h ^{61}Cu activities obtained by subtracting the shorter and longer half-life components from the data are also shown.

trons from the Faraday cup. Additional errors in the data are $\pm 6\%$ uncertainty in the photon flux, $\pm 4\%$ uncertainty in the efficiency of the NaI crystals for detecting the positron activities, and a composite of $\pm 3\%$ due to several miscellaneous sources.

The $(\gamma, 2n)$ cross section of ^{63}Cu was measured at photon energies of 22.2, 23.7, and 25.7 MeV with a photon-beam energy resolution of 3%. These measurements were limited to three representative energies because of the long irradiation and counting times required for the determination of the 3.3-h ^{61}Cu activity. The decay of a copper sample as a function of time after an irradiation with 25.6-MeV positrons striking the Be annihilation foil is presented in Fig. 10 as an example of the data. These data were collected in periods of 10 min, 1 h, or 3 h, depending on the time after the end of the irradiation. Also shown in Fig. 10 is the least-squares fit of the decay into three components, the 9.8-min activity from $^{63}\text{Cu}(\gamma, n)^{62}\text{Cu}$ reactions, the 3.3-h activity from $^{63}\text{Cu}(\gamma, 2n)^{61}\text{Cu}$ reactions, and the 12.8-h activity from $^{65}\text{Cu}(\gamma, n)^{64}\text{Cu}$ reactions. These components were obtained by means of the computer program CLSQ.¹⁹ The $^{63}\text{Cu}(\gamma, 2n)$ cross sections were calculated using the differences in the 3.3-h activities produced by the positron and electron bombardments and a value of 0.63 for the fraction of ^{61}Cu disintegrations which emit positron particles. This positron branching fraction was obtained from the decay scheme recently proposed by Schöneberg and Flammersfeld,²⁰ and the error in this fraction is estimated to be $\pm 12\%$. Corrections were applied to the $(\gamma, 2n)$ cross-section

¹⁹ J. B. Cumming, Brookhaven National Laboratory Report No. BNL-6470, 1962 (unpublished).

²⁰ R. Schöneberg and A. Flammersfeld, Z. Physik 200, 205 (1967).

TABLE I. $^{63}\text{Cu}(\gamma, 2n)$ cross sections. See text for a discussion of errors.

γ -ray energy (MeV)	Cross section (mb)
22.2	8.0 ± 0.5
23.7	10.0 ± 0.5
25.7	9.3 ± 0.5

data which were similar to those described above for the (γ, n) work; however, in this case the corrections for multiple scattering of photons within the copper samples was negligibly small. The resulting cross sections for the $^{63}\text{Cu}(\gamma, 2n)$ reaction are presented in Table I. The errors given in this table represent only the statistical uncertainties of the 3.3-h ^{61}Cu activity produced by positron annihilation photons. Other errors are $\pm 6\%$ due to uncertainties in the photon flux, $\pm 5\%$ due to the uncertainty in the efficiency of the NaI crystals for detecting the positron activities, the $\pm 12\%$ error in the positron branching fraction, and $\pm 3\%$ due to several miscellaneous sources.

DISCUSSION

Several measurements of the $^{63}\text{Cu}(\gamma, n)$ cross section have been performed with bremsstrahlung beams.²¹⁻²⁶ Values for the peak cross section derived from these measurements lie in the range 94–108 mb, and the energies at which the peaks were observed vary from 16.9 to 17.5 MeV. The present result for the peak cross section 75 ± 6 mb, is significantly lower than the bremsstrahlung data; however, the energy at which the peak cross section was observed (about 17.1 MeV) is consistent with the bremsstrahlung results. In an experiment using monoenergetic γ rays from a $^3\text{H}(p, \gamma)$ source and the activation method of detection, Del Bianco and Stephens⁹ measured a cross section of 52.5 ± 2.1 mb for the $^{63}\text{Cu}(\gamma, n)$ reaction at 20.5 MeV, a result which is significantly larger than the (γ, n) cross section of 37 ± 4 mb obtained in the present work. The (γ, n) cross section of ^{63}Cu has also been measured many times with 17.6- and 14.8-MeV γ rays from the $^7\text{Li}(p, \gamma)$ reaction. If one assumes the ratio of intensities of the 17.6- and 14.8-MeV γ rays is 2.1,²⁷ the equivalent cross section for Li γ rays calculated from the data presented in Fig. 9 is 63 ± 5 mb, which agrees well with the more recent Li γ -ray results of 62 ± 4 mb obtained by Yasumi *et al.*,⁶ and 59 ± 6 mb by Coote *et al.*⁷

Fultz *et al.*⁵ at Livermore have measured the $[(\gamma, n) + (\gamma, pn)]$ cross sections of the isotopes of copper

with a photon beam from a positron-photon monochromator similar to that described in this paper and with a 4π configuration of BF_3 counters and paraffin for detecting neutrons. For energies less than the $^{63}\text{Cu}(\gamma, pn)$ threshold (16.8 MeV), the $[(\gamma, n) + (\gamma, pn)]$ cross section of ^{63}Cu measured by the Livermore group can be compared directly with the results of the present investigation. The two sets of data are fairly similar except that the energy scales are displaced by a significant amount, e.g., the data of Fultz *et al.* peaks at roughly 16.6 MeV, or about 0.5 MeV less than the energy of the peak measured in this experiment. In view of the photon-beam energy resolutions of the two experiments, 3% for Fultz *et al.* and 2% for the present measurement, this energy difference does not present a serious discrepancy; nevertheless, on the basis of the photon-beam spectrum measurement and the energy calibration at 15.1 MeV, together with the good agreement between the $^{63}\text{Cu}(\gamma, n)$ threshold energy observed in this experiment and the calculated threshold, we believe that the energy scale of the present data is correct to within $\pm \frac{3}{4}\%$. For comparison of the present (γ, n) results with the $^{63}\text{Cu}[(\gamma, n) + (\gamma, pn)]$ data of Fultz *et al.*, which is presented in Fig. 11, the latter data were shifted upward in energy by 2.7%. The error bars shown in Fig. 11 include the statistical uncertainties in the neutron-yield measurements of Fultz *et al.* and the statistical uncertainties in the present activation determinations as well as the uncertainties in the present Faraday-cup correction. The over-all uncertainty in the peak of the cross section measured by Fultz *et al.* is about $\pm 10\%$ and in the peak of the present measurement is about $\pm 8\%$. The peak cross section obtained in this experiment exceeds that given by Fultz *et al.* by about 7%, or slightly less than the over-all uncertainty of each of the measurements. The two results would agree better if, in the present work, the measured photon flux had been utilized instead of the Monte Carlo calculations.

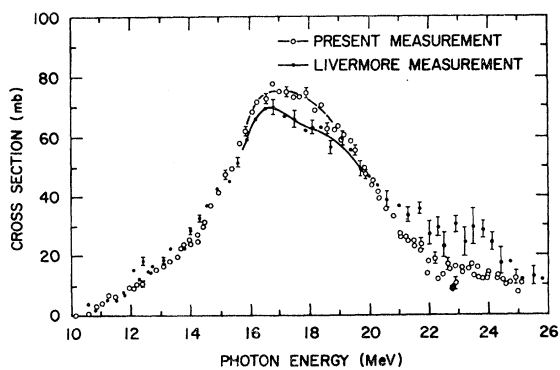


FIG. 11. The $^{63}\text{Cu}(\gamma, n)$ cross section from the present measurement and the $^{63}\text{Cu}(\gamma, n) + (\gamma, pn)$ cross section from the measurement by Fultz *et al.* at Livermore (Ref. 5). The latter data were shifted upward in energy by 2.7% to normalize the results to the present measurement. The error bars shown do not include systematic errors. See text for a discussion of errors.

²¹ P. R. Byerly and W. E. Stephens, Phys. Rev. **83**, 54 (1951).

²² B. C. Diven and G. M. Almy, Phys. Rev. **80**, 407 (1950).

²³ H. E. Johns, L. Katz, R. A. Douglas, and R. N. H. Haslam, Phys. Rev. **80**, 1062 (1950).

²⁴ A. I. Berman and K. L. Brown, Phys. Rev. **96**, 83 (1954).

²⁵ V. F. Krohn and E. F. Shrader, Phys. Rev. **87**, 685 (1952).

²⁶ M. B. Scott, A. D. Hanson, and D. W. Kerst, Phys. Rev. **100**, 209 (1955).

²⁷ V. Meyer, H. Muller, H. H. Staub, and R. Zurmuhle, Nucl. Phys. **27**, 284 (1961).

In Fig. 12 the present $^{63}\text{Cu}(\gamma, 2n)$ cross-section data are compared with the results from Fultz *et al.*⁵ As in the above comparison of the (γ, n) cross sections, the latter data have been shifted upward in energy by 2.7%. The error bars shown in Fig. 12 include only the statistical uncertainties in the measurements. Although measurements were performed at only three energies in the present experiment, it is evident that the data of Fultz *et al.* are consistently higher than the present cross sections by approximately 30%. This difference is somewhat larger than might be expected, considering that the over-all uncertainties in both measurements are roughly $\pm 15\%$.

The $^{63}\text{Cu}(\gamma, pn)$ cross section has been derived by normalizing the $[(\gamma, n) + (\gamma, pn)]$ cross section of Fultz *et al.*, as presented in Fig. 11, to the present (γ, n) cross section just below the (γ, pn) threshold and then subtracting the two sets of data. The resulting $^{63}\text{Cu}(\gamma, pn)$ cross-section data are shown in Fig. 13. The error bars reflect the statistical uncertainties in the data from which the (γ, pn) cross section was derived, and the dashed curves show the shift from the solid curve allowed by the possible energy-dependent systematic error of Fultz *et al.* which resulted from the bremsstrahlung subtraction procedure.²⁸ A further error of $\pm 8\%$ is mainly a result of uncertainties in the flux and detector efficiencies. Above the threshold energy, the (γ, pn) cross section rises quite slowly, as might be expected because of the Coulomb barrier, reaches a peak of 15 mb at roughly 23 MeV, and then decreases.

A summary of the integrated cross sections up to 25 MeV that were obtained in this study, together with

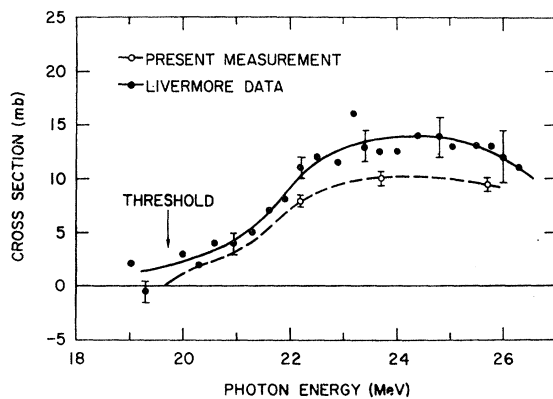


FIG. 12. The $^{63}\text{Cu}(\gamma, 2n)$ cross section from the present measurement and from the measurement by Fultz *et al.* at Livermore (Ref. 5). The latter data were shifted upward in energy by 2.7% as explained in the caption of Fig. 11. The error bars include only the statistical uncertainties in the yield measurements. See text for a discussion of the errors. The dashed curve through the present data was used in the integration and is drawn on the basis of the data points, the threshold energy, and the shape of the Livermore data.

²⁸ The estimate of this systematic error was supplied by R. L. Bramblett.

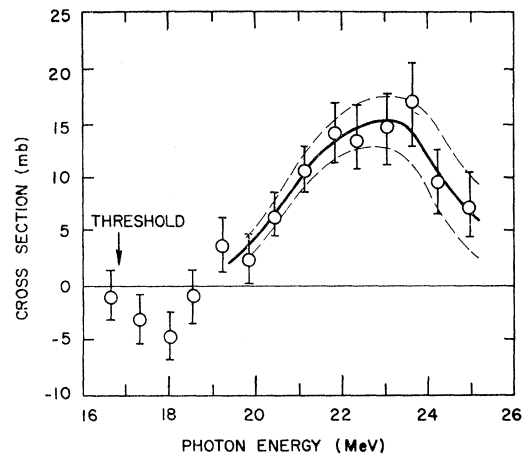


FIG. 13. The $^{63}\text{Cu}(\gamma, pn)$ cross section derived from the present (γ, n) measurement and from the $(\gamma, n) + (\gamma, pn)$ measurement by Fultz *et al.* (Ref. 5). See text for a discussion of the dashed curves and of the error bars.

those derived from the data of Fultz *et al.*, is given in Table II. The total integrated cross sections represent the sum of the integrals of only the partial cross sections given in the table. The integrated cross sections obtained at Livermore for a large number of nuclei have typically agreed with the results of the dipole sum rule with no exchange force contribution. Since the present results are only somewhat higher than the Livermore ^{63}Cu results, they tend to verify that any exchange-force term is small.

Except for (γ, p) cross section, the sum of the (γ, n) and $(\gamma, 2n)$ cross sections measured in this study and of the (γ, pn) cross section derived from the present data and the data of Fultz *et al.* represents the total photon absorption cross section. This sum and the absorption cross section calculated for copper by Huber *et al.*¹ using the dynamic collective theory for spherical nuclei are shown in Fig. 14. A similar calculation for the cross section of ^{63}Cu should result in the same general features as those for the cross section of natural copper shown in the figure. The theoretical

TABLE II. Integrated photoreaction cross sections of ^{63}Cu up to 25 MeV.

Experiment	Reaction	Integrated cross section (MeV mb)	Total (MeV mb)
Present	(γ, n)	490 ± 40	586 ± 67
	$(\gamma, 2n)$	36 ± 12^a	
	(γ, pn)	60 ± 15^b	
Fultz <i>et al.</i>	$(\gamma, n) + (\gamma, pn)$	515 ± 52^c	563 ± 57
	$(\gamma, 2n)$	48 ± 5^d	

^a Based on the dashed curve in Fig. 12.

^b Derived from (γ, n) data of present work and $[(\gamma, n) + (\gamma, pn)]$ data of Fultz *et al.* (Ref. 5).

^c Energy scale of these data (Ref. 5) shifted by the factor 1.027. Without the shift the result is 511 ± 51 .

^d Energy scale of these data (Ref. 5) shifted by the factor 1.027. Without the shift the result is 56 ± 6 .

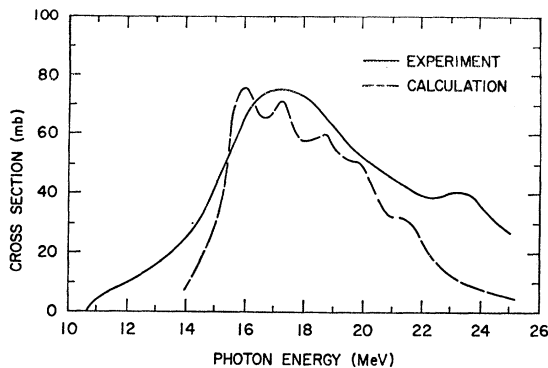


FIG. 14. The $^{63}\text{Cu}(\gamma,n) + (\gamma,2n) + (\gamma,pn)$ cross section from the present measurement and the calculated absorption cross section for natural copper (from Ref. 1).

cross section does not include the "direct" (γ,n) cross section which has been estimated to be only about 10% of the total absorption cross section.⁵ It is evident that the magnitude and the gross features of the theoretical cross section between 15 and 21 MeV agree fairly well with the experimental data; however, the predicted fine structure in the region of the peak of the giant resonance was not observed in this experiment, and the width of the giant-resonance indicated by the calculated cross section is appreciably less than the measured width ~ 9 MeV at half the maximum cross section. Recently Drechsel, Seaborn, and Greiner²⁹ have calculated the giant-resonance cross sections of a few nuclei by treating the dipole states in the particle-hole framework (instead of the hydrodynamic model) and describing the surface vibrations with the collective model. This method spreads the giant resonance over a broader spectrum of states than does the dynamic collective model, and might therefore better predict the ^{63}Cu photoabsorption cross section.

The only significant structure observed in the experimental cross section in Fig. 14 other than the main giant resonance is a small bump which is centered at about 23 MeV. This bump is mostly due to the (γ,pn) cross section, which has an integrated cross section of about 10% of the total integrated cross section. A possible explanation of this satellite resonance is the isobaric splitting of the dipole states which has been proposed by Fallieros, Goulard, and Venter,³⁰ and by

others.³¹⁻³³ According to Fallieros *et al.*,³⁰ the coupling of a particle-hole pair to a specific four-quasiparticle excitation should split the particle-hole dipole state into a higher-lying analog state (with isobaric spin $T+1$) and a somewhat modified version of the original particle-hole state (isobaric spin T). The decay of the $(T+1)$ analog resonance to the $(T-\frac{1}{2})$ ground state or $(T-\frac{1}{2})$ excited states is inhibited according to isobaric selection rules. The extent of such decay processes is influenced by the amount of isobaric spin mixing in the compound state. Proton decay from the analog resonance to the $T+\frac{1}{2}$ states of the residual nucleus is allowed. The calculations for ^{90}Zr predict that the analog state for this nucleus should be located at an energy of about 5 MeV higher than its lower-lying counterpart, and should have approximately 20% of the total dipole strength.³⁰ In measurements of the $(\gamma,n) + (\gamma,pn) + (\gamma,2n)$ neutron cross sections of ^{89}Y , ^{90}Zr , and ^{91}Zr , Berman *et al.*³⁴ observed structure on the high-energy side of the giant resonance which they suggest may be associated with the isobaric analog states predicted by Fallieros *et al.* In the case of ^{63}Cu , the energy difference between the analog state and the main peak of the giant resonance should, according to the expression given by Fallieros *et al.*, be about 6.6 MeV, which compares favorably with ~ 6 MeV obtained from the experimental data given in Fig. 14.

ACKNOWLEDGMENTS

We wish to thank A. Dolinski for helping with the experimental apparatus, D. E. Houston for computer programming, Dr. J. R. Beyster for his encouragement in these measurements, and many others at Gulf General Atomic Accelerator Physics Department who contributed to this experiment. We are indebted to Dr. G. Merkel for helpful discussions on the determination of the efficiency of the NaI crystals for detecting the positron activities, to G. Buzzelli and Dr. D. Barr for valuable aid in the determination of the efficiency of this detector, and to Dr. L. S. Cardman and Dr. R. O. Owens for sending us their Monte Carlo code for calculating the positron annihilation flux. We further acknowledge valuable discussions with Dr. B. L. Berman, Dr. W. R. Gibbs, Dr. R. L. Bramblett, and Dr. S. C. Fultz concerning the interpretation and comparison of the data.

³¹ V. V. Balashov and E. L. Yadrovsky, *Phys. Letters* **22**, 509 (1965).

³² H. Morinaga, *Z. Physik* **188**, 182 (1965).

³³ A. Piazza, H. G. Wahsweiler, and W. Greiner, *Phys. Letters* **25B**, 579 (1967).

³⁴ B. Berman, J. Caldwell, R. Harvey, M. Kelly, R. Bramblett, and S. Fultz, *Phys. Rev.* **162**, 1098 (1967).

²⁹ D. Drechsel, J. B. Seaborn, and W. Greiner, *Phys. Rev.* **162**, 983 (1967).

³⁰ S. Fallieros, B. Goulard, and R. H. Venter, *Phys. Letters* **19**, 398 (1965).